J Electroceram (2009) 23:415–421
DOI 10.1007/s10832-008-9480-8

Effect of fluorine doping on the properties of ZnO films deposited by radio frequency magnetron sputtering

D. Y. Ku · Y. H. Kim · K. S. Lee · T. S. Lee · B. Cheong · T.-Y. Seong · W. M. Kim

Received: 29 May 2007 / Accepted: 18 March 2008 / Published online: 12 April 2008

Abstract ZnO films with varying fluorine content were prepared on Corning glass by radio frequency magnetron sputtering of ZnO target containing ZnF_2 at room temperature, and the compositional, electrical, optical, and structural properties of the as-grown films together with the vacuum-annealed films were investigated. The fluorine content in the fluorine doped ZnO (FZO) films increased almost linearly with increasing ZnF_2 content in sputter target, and the highest atomic concentration was 7.3%. Vacuum-annealing caused a slight reduction of fluorine content in the films. The resistivity of the as-grown FZO films deposited showed a typical valley-like behavior with respect to the fluorine content in film, i.e. having minimum resistivity at intermediate fluorine content. Despite high fluorine content in the FZO films, the carrier concentration remained below 1.2×10^{20} cm^{-3}, leading to very low doping efficiency level. Upon vacuum-annealing, the resistivity of FZO films decreased substantially due to increase in both the carrier concentration and the Hall mobility. From the structural analysis made by X-ray diffraction study, it was shown that addition of small amount of fluorine enhanced the crystallinity of FZO films with (002) preferred orientation, and that large amount of fluorine addition yielded disruption of preferred orientation. It was also shown that doping of fluorine rendered a beneficial effect in reducing the absorption loss of ZnO films in visible range, thereby substantially enhancing the figure of merit.

Keywords Fluorine doped ZnO film · Transparent conducting oxide · Magnetron sputtering · Vacuum-annealing

K. S. Lee · T. S. Lee · B. Cheong · W. M. Kim (✉)
Thin Film Materials Research Center,
Korea Institute of Science and Technology,
39-1, Hawolgok-dong, Sungbuk-gu,
Seoul 136-791, South Korea
e-mail: wmkim@kist.re.kr

Y. H. Kim · T.-Y. Seong
Division of Materials Science and Engineering, Korea University,
5-1, Anam-Dong, Sungbuk-gu,
Seoul 136-701, South Korea

D. Y. Ku
Il Dong Chemical Co., Ltd.,
310, Gongdan-dong,
Gumi, Kyeongsangbuk-do 730-906, South Korea

1 Introduction

Transparent conducting oxide (TCO) films are materials which are highly transparent to visible light and electrically conducting. TCO films have been used in many applications as transparent electrodes of flat panel devices, solar cell and IR reflectors. Recently, ZnO films doped with metallic ions have drawn a great deal of attention as an alternative for the most widely used Sn doped In_2O_3 films due to recent soar in raw material cost of indium [1]. Impurity doped ZnO films are attractive TCOs due to their low material cost, non-toxicity and stability under hydrogen plasma together with low resistivity and high visible transmission [2, 3]. Most of the related studies have been focused on the Al doped ZnO [4, 5] and the Ga doped ZnO films due to their low electrical resistivity [6, 7]. Unlike the abundant studies on ZnO films doped with cation dopants such as Al or Ga, only a few investigations in which fluorine was used as anion dopant can be found in literature. Fu et al. obtained a noteworthy result by doping fluorine to ZnO (FZO) films using a chemical vapor deposition (CVD) technique, in which electrical resistivity of 6×10^{-4} Ωcm and Hall mobility as high as 40 cm^2/Vs were reported [8]. Chemical spray method was utilized to

fabricate FZO films by Olivera et al. [9, 10], but the electrical properties were poorer than those obtained by CVD. Only study on FZO films deposited using physical vapor deposition technique can be found in the work of Miyata et al. [11, 12]. They reported the possibility of fabricating fluorine doped ZnO with better electrical properties by using vacuum arc plasma evaporation. On the other hand, Xu et al. [13] reported that FZO films with low electrical resistivity of 7.95×10^{-4} Ωcm and good optical transparency could be prepared by a controlled annealing of ZnF_2 films, which were deposited by electron-beam evaporation, in oxygen atmosphere.

Gordon [14] stated in his review article that, unlike cation dopants which perturbs conduction band, the fluorine dopant mainly perturbs the valence band, thereby leaving the conduction band relatively free of scattering, which would lead to high mobility as well as low absorption loss in FZO films. Despite such beneficial effects of fluorine doping, no study has been reported on the fluorine doped ZnO films by using sputtering technique which has been widely used for fabrication of TCO films. In this study, fluorine doped ZnO films were deposited by radio frequency (rf) magnetron sputtering of ZnO targets containing ZnF_2 at room temperature, and their compositional dependence of the electrical, optical and structural properties were examined. Also, the changes in the corresponding properties upon vacuum-annealing were analyzed.

2 Experimental details

FZO films with varying fluorine content were deposited on glass substrates (Corning Eagle) by rf magnetron sputtering of 2-in. target. The fluorine doping was done by sputtering ZnF_2 containing ZnO targets (0, 1.3, and 10 wt.% ZnF_2). FZO films with six different fluorine content were prepared by either sputtering single target or co-sputtering of two targets with different ZnF_2 composition, and the target composition and the respective rf power used for each sample are listed in Table 1. The estimated ZnF_2 content of co-sputtered film was calculated from the pre-determined deposition rates by using theoretical densities of ZnO and ZnF_2 [15], and by assuming that all the fluorine atoms in target were incorporated into the films in the form of ZnF_2.

Film thickness was kept at around 200 nm for all the films by controlling the deposition time according to the predetermined deposition rates which were measured from the films deposited on strip-masked substrates using a profilometer. The base pressure in the chamber was below 5×10^{-5} Pa, and the sputtering deposition was carried out at a pressure of 0.13 Pa. The distance between the target and the substrate was 50 mm. The substrate was not intentionally heated, and rotated at a constant speed of 12 rpm during sputtering. Annealing experiment was performed in rapid thermal processing chamber which can be pumped down to below 10^{-4} Pa. Annealing treatments of the as-prepared films were carried out in vacuum of 10^{-4} Pa for 1 h. The usual annealing temperature was 300 °C unless specified otherwise.

For compositional analysis, Auger electron spectroscopy (AES) analysis was carried out. In order to make quantitative analysis, composition analysis by using Rutherford backscattering spectrometry was performed on FZO film deposited by sputtering ZnO target with highest ZnF_2 content of 10 wt.%, i.e. having the highest fluorine content among all samples. And the very same sample was then analyzed by using AES. By comparing both results, the sensitivity factor of each element was determined, and used for other AES analysis. The electrical resistivities, Hall mobilities, and carrier concentrations were determined from Hall-effect measurement equipment using a Van der Pauw method. The structural analysis was carried out by an X-ray diffraction (XRD) measurement (CuK_α wavelength = 1.540562 Å, $\theta-2\theta$ scan mode). The optical transmission and reflection spectra were obtained from a ultraviolet-visible spectrophotometer in wavelength ranges of 250~1,100 nm.

3 Results

3.1 Electrical properties

Figure 1 summarizes (a) the electrical resistivities, (b) the Hall mobilities, and (c) the carrier concentrations of the undoped ZnO and FZO thin films plotted against ZnF_2 content in targets. The resistivity of the as-grown FZO films deposited at room temperature showed a typical valley-like behavior, i.e. having minimum resistivity at intermediate fluorine content. Small addition of ZnF_2 resulted in fairly large increase in both Hall mobility and carrier concentration. As-grown FZO2 film deposited with target containing 1.3 wt.% ZnF_2 gave the highest Hall mobility of about 26.4 cm^2/Vs together with the maximum carrier concentration of 1.13×10^{20} cm^{-3}. Vacuum-annealing of the FZO films resulted in large drop of resistivity, especially for films with large fluorine content, due to increase of both the free carriers and the Hall mobility. The Hall mobility value as high as 39.2 cm^2/Vs was observed for FZO2 film. Although the carrier concentration increased after annealing in vacuum, the absolute values were still remained at relatively low level, the highest carrier concentration being still less than $\sim3\times10^{20}$ cm^{-3}.

3.2 Compositional properties

Shown in Fig. 2 are the variations of fluorine content in the as-deposited and the vacuum-annealed FZO films measured

Table 1 List of target composition used and the respective rf power applied to prepare FZO films with different fluorine contents.

Samp1e ID	rf power (W)			Estimated ZnF_2 in target[a] (wt.%)
	ZnO	ZnO–ZnF_2 (1.3 wt.%)	ZnO–ZnF_2 (10 wt.%)	
ZnO	50	–	–	0
FZO1	50	50	–	0.68
FZO2	–	50	–	1.3
FZO3	–	50	20	2.71
FZO4	–	50	50	4.13
FZO5	–	–	50	10

[a] Calculated values from the pre-determined deposition rates by using theoretical densities of ZnO and ZnF_2, and by assuming that all the fluorine atoms in target were incorporated into the films in the form of ZnF_2.

for FZO2, FZO3, and FZO5 samples by AES with respect to the estimated fluorine content which would be attained if all the fluorine atoms in target were incorporated into the films. For the as-grown FZO films, the fluorine contents in films increased almost linearly with increasing fluorine contents in targets, although they were slightly lower than those in target. Vacuum annealing resulted in the reduction of fluorine content, the extent of decrease in fluorine content being larger for the films with larger fluorine contents in the as-deposited states. In an experiment, FZO5 films were deposited at elevated temperature of 250 °C, and its composition is also presented in Fig. 2. The fluorine content of FZO5 film deposited at the substrate temperature of 250 °C yielded only 1.5 at.%, while that deposited at room temperature using the same target being as high as 7.3 at.%. A similar temperature dependence of fluorine incorporation was observed in sputter deposited In_2O_3 films [16], but the temperature effect was not so pronounced as was observed in this study for ZnO films.

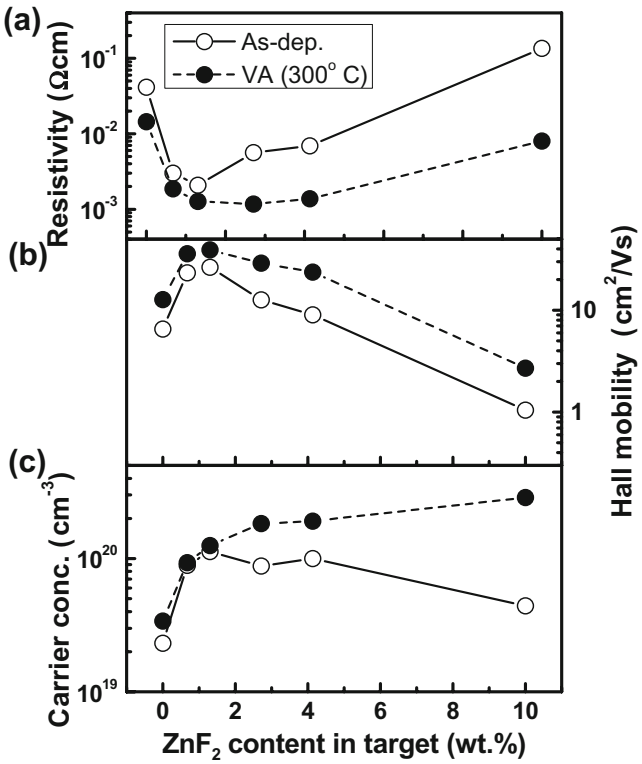

Fig. 1 Electrical properties of the as-deposited and the vacuum-annealed ZnO and FZO films, (**a**) resistivities, (**b**) Hall mobilities, and (**c**) carrier concentrations

3.3 Optical properties

In Fig. 3(a), the transmittance spectra obtained for ZnO, FZO2 and FZO5 films in the as-deposited (solid lines) and the vacuum annealed (dashed lines) states are compared. It is clear that the addition of fluorine caused the overall increase in visible transmission as well as the shift of absorption edge toward higher energy side. For a given composition, vacuum-annealing also resulted in a similar

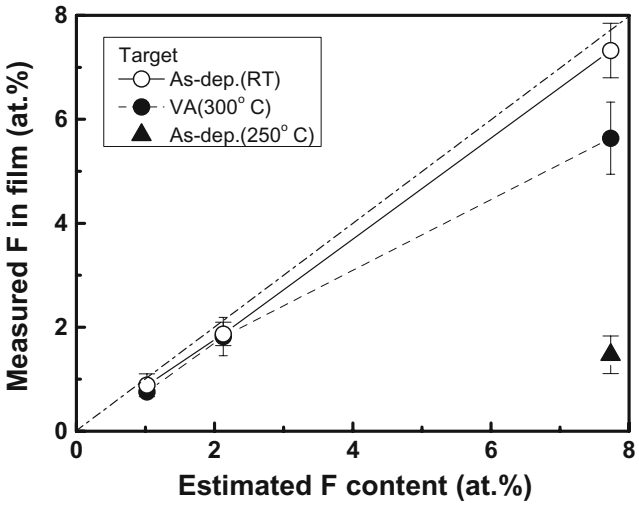

Fig. 2 Fluorine contents in FZO2, FZO3 and FZO5 films with respect to estimated fluorine content which would be attained if all the fluorine atoms in target were incorporated into the films. *Open circles with solid line*, *closed circles with dashed line*, and *open triangles with solid lines* represent the as-deposited films at room temperature, the vacuum-annealed films deposited at room temperature, and as-deposited at 250 °C, respectively

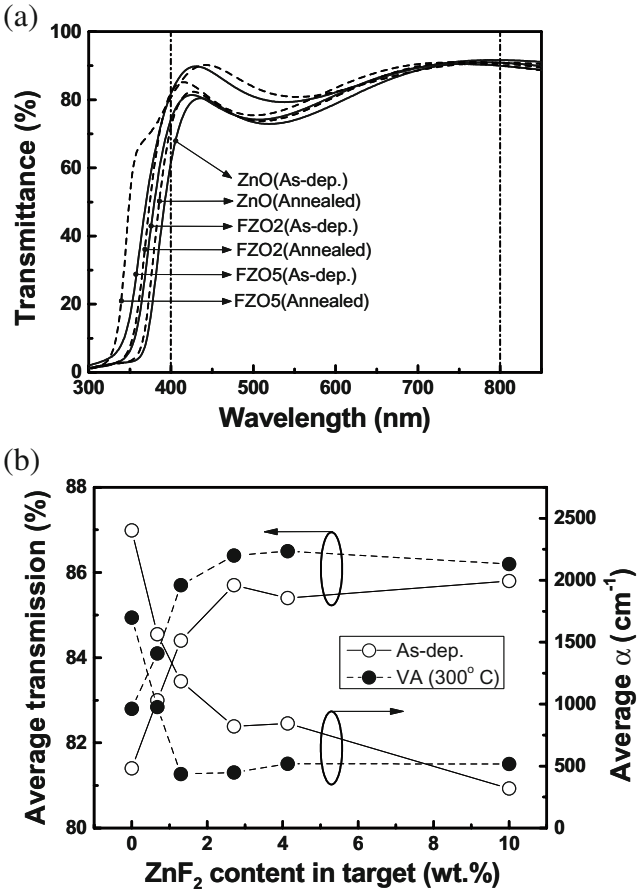

Fig. 3 (**a**) Optical transmission spectra of the as-deposited (*solid*) and the vacuum-annealed (*dashed*) ZnO and FZO2, and FZO5 films. The *vertical dash-dot lines* shown at 400 and 800 nm are draw for eye-guide to clarify the averaged range. (**b**) Variations of the average transmission and absorption coefficient. *Open circles with solid line*, *closed circles with dashed line* represent the as-deposited films and the vacuum-annealed films, respectively

optical behavior, i.e. the overall increase in visible transmission as well as the shift of absorption edge toward higher energy side. Figure 3(b) shows a plot of the transmittance and the absorption coefficient averaged in visible range of 400~800 nm. At low fluorine content, the average transmittance increased sharply, then saturated. Upon vacuum-annealing, the average transmittance increased by about 1% for all the films. Although it is evident that addition of fluorine to ZnO films led to enhanced transmittance, the beneficial effect of using fluorine dopant can be found more clearly by examining the absorption loss. The absorption coefficient, α, was calculated from the spectroscopic optical data by adopting relationship which is defined with corrections for reflection loss at the front surface of the sample, i.e., $\alpha = (1/d)\ln[(1-R)/T]$, where d, T and R are the film thickness, transmission and reflection, respectively [17]. For the as-deposited films, the average absorption coefficient kept decreasing with increasing fluorine content. And, after vacuum-annealing, the films with larger fluorine content than FZO1 film exhibited very low average absorption coefficient of about 500 cm^{-1}.

From Fig. 3(a), fairly large shift of the absorption edge toward the higher energy side (blue-shift) can be seen with increasing fluorine content. In order to examine the shift of absorption edge with respect to fluorine content, direct allowed band-gaps of ZnO and FZO films were evaluated by using the relation of $\alpha h\nu \propto \left(h\nu - E_g\right)^{1/2}$ (for $h\nu > E_g$), where h is Planck's constant, ν the frequency, and E_g the band-gap [18]. The optical band-gaps of ZnO and FZO films, which were estimated by plotting $(\alpha h\nu)^2$ vs. $h\nu$ and extrapolating the linear portion near the onset of absorption edge to the energy axis, are plotted in Fig. 4 as a function of carrier concentration. General behavior of the optical band-gap can be categorized into three groups, as marked by dashed circles in the plot, depending on the band-gap energy level in relation to the carrier concentration; (1) group 1 films with low fluorine content like FZO1 and FZO2 including ZnO, (2) group 2 films with intermediate fluorine content like FZO3, and (3) group 3 films with large fluorine content like FZO4 and FZO5. For each group, the optical band-gap exhibited an increasing tendency with increasing carrier concentration, showing a typical Burstein–Moss (BM) shift. For a given carrier concentration range, however, the level of optical band-gap was the highest for group 3 films and the lowest for group 1 films.

3.4 Structural properties

Figure 5(a) contains XRD profiles of the as-deposited and the vacuum-annealed ZnO and FZO films. Pure ZnO film showed only peak from (002) plane indicating a typical wurtzite structure with (002) preferred orientation. With small addition of ZnF_2, peak intensity from (002) plane increased, showing maximum intensity for FZO2 film. This

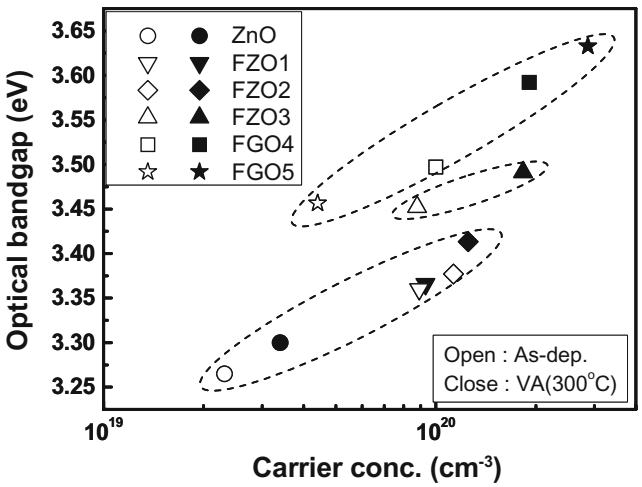

Fig. 4 Behavior of the optical band-gaps shown in relation to the carrier concentrations in films

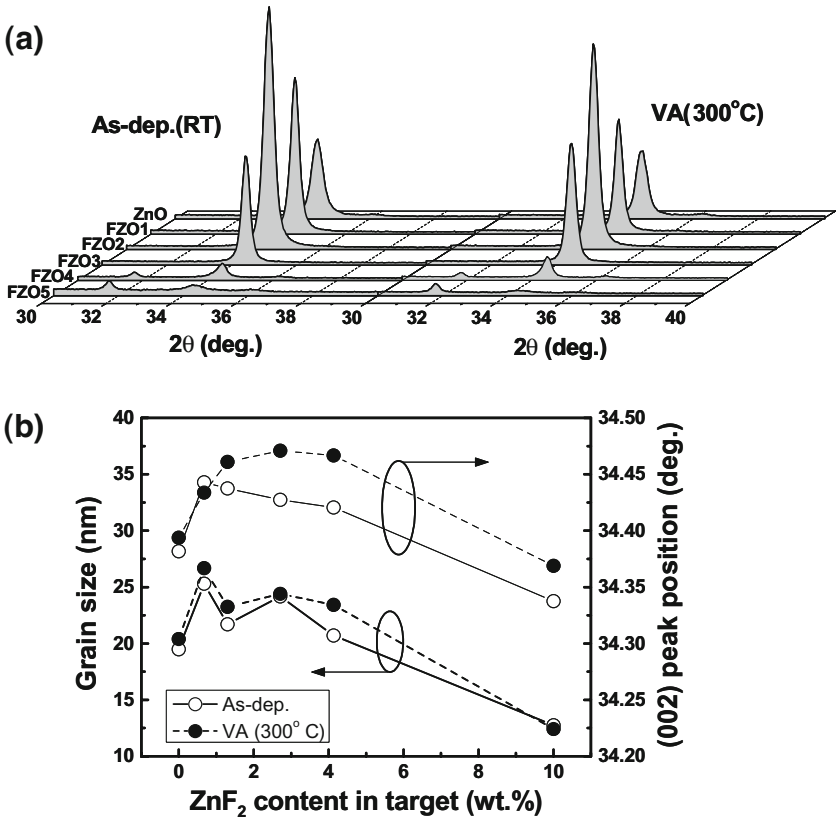

Fig. 5 (**a**) XRD profiles of the as-deposited and the vacuum-annealed ZnO and FZO films. (**b**) Variations of the grain size and (002) peak position

is consistent with the observation that dopant or impurity like Al acted as a mineralizer or surfactant which improves texturing of growing ZnO film [19]. With further increasing fluorine content, the intensity of (002) peak diminished, instead the weaker peaks from (100) and (101) planes together with (110) peak (not shown in the plot) appeared. Vacuum-annealing did not induce any appreciable change in film structure. In Fig. 5(b), the variations in grain size and (002) peak position are shown. The grain size was derived from the integral width of the (002) line according to the Scherrer formula by taking into account the instrumental peak broadening. The grain sizes were in the range from 19 to 25 nm except for the FZO5 film which had the smallest grain size of about 12 nm. Upon vacuum-annealing, rather small but noticeable increase in grain sizes of about 1~2 nm was observed. The (002) peak position of the as-deposited films decreased toward lower angle side with increasing fluorine content, indicating the expansion of c-axis lattice parameter. Upon annealing, except for FZO1 film, the (002) peak position moved toward the higher angle side.

4 Discussion

Doping efficiency can be evaluated by taking the ratio of the free carrier concentration to the atomic fluorine concentration, assuming that the free carriers are originated solely from the substituted fluorine atoms [8]. It was reported that ZnO films grown by CVD technique at elevated temperature had fluorine content less than 1 at.% [8, 20]. But FZO films grown by CVD had moderate carrier concentration of $2\sim4\times10^{20}$ cm^{-3}, leading to doping efficiency as high as 0.97 [8]. On the other hand, the calculated doping efficiencies of the as-deposited FZO2, FZO3 and FZO5 films were 0.15, 0.06, and 0.007, respectively. Even after vacuum-annealing, the corresponding values of doping efficiency were merely 0.2, 0.11 and 0.06, respectively. Considering that ZnO film is known to possess usually such native donors as oxygen vacancies and zinc interstitials, the actual doping efficiency would be substantially lower than the calculated ones. The low doping efficiency observed in our films is ascribed to the non-equilibrium nature of sputter-deposition. Unlike CVD process, in which the deposition follows an equilibrium path, incorporation of fluorine into the growing film is forced in sputter deposition process. This would lead to an increased probability of fluorine atoms to be incorporated into films in the form of interstitials, compound like ZnF_2 phase and/or grain boundary segregation instead of substituting the oxygen. The decrease of (002) peak position with increasing fluorine content observed in as-deposited FZO films and the relatively large shift of (002) peak position toward the higher angle position observed for the vacuum-annealed FZO films

might support the removal of fluorine interstitials upon vacuum annealing.

The increase in the carrier concentration as well as the Hall mobility upon vacuum-annealing is attributed to the filling-in oxygen vacancies by fluorine interstitials. It was reported in the first-principles pseudopotential calculation on ZnO that, in oxygen deficiency condition, oxygen vacancies have lower energy than zinc interstitials and hence should be more abundant [21]. Since our films were deposited without intentional addition of oxygen into the sputter gas, the films will show a tendency of oxygen deficiency. It is known that the creation of doubly charged oxygen vacancy is not as effective as singly charged doping due to low mobility [22]. Furthermore, the fluorine interstitials, if present, would attract free electrons due to the high electronegativity of fluorine, i.e. act as charge trap sites, resulting in decrease of the carrier concentration. Therefore, the filling-in oxygen vacancies by fluorine interstitials upon vacuum-annealing will lead to increase of the free carriers as well as the Hall mobility as was observed in this study.

The larger optical band-gap observed in FZO4 and FZO5 films with higher fluorine contents cannot be explained by the BM shift. Although blue-shift in nano-sized semiconductors by quantum confinement effect was proposed by Brus [23], the grain size of even FZO5 film is too large to consider the quantum confinement effect as the reason of blue-shift. One can think of formation of open structure with large grain boundaries due to small grain size, but this cannot provide full explanation for FZO4 films with similar grain size to FZO2 and FZO3 films. Other possibilities are either formation of secondary phase like ZnF_2 by some excess fluorine atoms or segregation of fluorine atoms at the grain boundaries. ZnF_2 is known as a wide band-gap insulator [24]. Although no report has been made on the band-gap energy of ZnF_2, the optical band-gap of ZnF_2 is thought to be near or higher than 5 eV judging from the transmission data of evaporated ZnF_2 film [13]. During deposition of FZO films with high fluorine content, excess fluorine may be adsorbed (both chemically and physically) on the growing surface, hindering further growth of ZnO crystallites. This would result in smaller grain size as well as possible disruption of crystal growth with preferred orientation. And the adsorbed fluorine atoms during deposition might exist as the adsorbed states by filling in the dangling bonds at the grain boundaries or segregated states.

From the above discussion, it seems that excess fluorine atom at high fluorine content in sputter target is incorporated in the form of interstitials, compound like ZnF_2 phase, adsorbed states and/or grain boundary segregation. Some of the interstitial fluorine atoms can be removed upon annealing by either filling-in oxygen vacancies or diffusing out to the grain boundaries. And some of the adsorbed fluorine at the grain boundaries might be removed during annealing from the film by grain boundary diffusion. The behavior of the optical band gap might have provided a clue that the some of the excess fluorine could be formed a second phase like ZnF_2 with high band gap energy. But, unfortunately, XRD analysis did not give any evidence of presence of secondary phase like ZnF_2 phase. More detailed study will be necessary to find out the exact form of excess fluorine and its chemical state in FZO films in the future.

It was evident that addition of fluorine to ZnO films led to enhanced transmittance as well as the lowered absorption loss. The beneficial effect of using fluorine dopant can be found more clearly by examining the figure of merit (FOM). The quantitative measure for the dimensionless FOM is defined by $FOM=1/\rho\alpha$ where ρ is the specific resistivity [25]. In Fig. 6, the calculated FOM of FZO films are plotted. Vacuum-annealed FZO2 and FZO3 films gave FOM values close to 2, which is fairly high considering that the resistivity remained in 10^{-3} Ωcm order range even for these films. Considering the beneficial effect of fluorine doping into ZnO such as low light scattering, i.e. low absorption loss and high Hall mobility, further search for a proper method of increasing doping efficiency in FZO films formed by sputtering would provide a possibility of obtaining excellent TCO films.

5 Conclusions

In this work, fluorine doped FZO films were prepared on Corning glass by rf magnetron sputtering of ZnO targets containing ZnF_2 at room temperature. Increase in ZnF_2 content in target resulted in increase of fluorine content in FZO films. Despite high fluorine content, all the as-grown FZO films exhibited relatively low level of the carrier

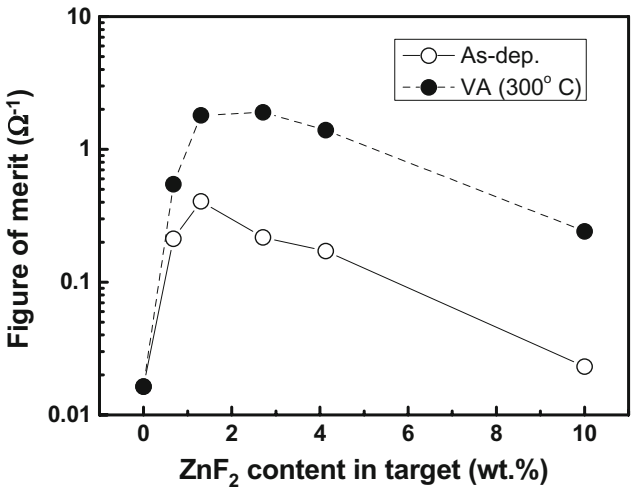

Fig. 6 Calculated figures of merit for the as-deposited and the vacuum-annealed ZnO and FZO films

concentrations, leading to very low doping efficiency. Undoped ZnO and FZO films with low fluorine content exhibited a typical hexagonal wurtzite structure with (002) preferred orientation, and FZO4 and FZO5 films with high fluorine content revealed polycrystalline fine structure. Vacuum-annealing of FZO films deposited at room temperature resulted in improved electrical resistivities largely due to enhancement of the carrier concentration together with increase in Hall mobility. No appreciable structural change was observed except for the small increase in the grain size and (002) peak shift toward higher angle side. It was perceived that large portion of fluorine atoms incorporated into the as-deposited ZnO films might exist in the form of interstitials, compound like ZnF_2 phase, adsorbed states and/or segregated states at the grain boundaries while only a little amount being substituted for oxygen atoms. It was shown that addition of fluorine to ZnO films resulted in substantial reduction of absorption coefficient in visible range, and that vacuum-annealing yielded FZO films with resistivity of about 1.2×10^{-3} Ωcm combined and with average absorption coefficients lower than 500 cm^{-1}. The beneficial effect of low absorption loss combined with high Hall mobility obtained for FZO films can be further utilized if a proper way of enhancing doping efficiency, i.e. carrier concentration, is sought in the future studies.

Acknowledgements This study was partially supported by a grant from the Fundamental R&D Program for Core Technology of Materials funded by the Ministry of Commerce, Industry and Energy, Republic of Korea.

References

1. J. F. Carlin Jr., *U.S. Geological Survey, Mineral Commodity Summaries*, Jan. (2006)
2. K. Ellmer, J. Phys. D: Appl. Phys. **34**, 3097 (2001). DOI 10.1088/0022-3727/34/21/301
3. T. Minami, MRS Bull. **25**(8), 38 (2000)
4. J. Kr, M. Zeman, O. Kluth, F. Smole, M. Topi, Thin Solid Films **426**, 296 (2003). DOI 10.1016/S0040-6090(03)00006-3
5. R. Groenen, J.L. Linden, H.R.M. van Lierop, D.C. Schram, A.D. Kuypers, M.C.M. van de Sanden, Appl. Surf. Sci. **173**, 40 (2001). DOI 10.1016/S0169-4332(00)00875-8
6. S.-M. Park, T. Ikegami, K. Ebihara, Thin Solid Films **513**, 90 (2006). DOI 10.1016/j.tsf.2006.01.051
7. S. Kishimoto, T. Yamada, K. Ikeda, H. Makino, T. Yamamoto, Surf. Coat. Technol. **201**, 4000 (2006). DOI 10.1016/j.surfcoat.2006.08.009
8. J. Hu, R.G. Gordon, Solar Cells **30**, 437 (1991). DOI 10.1016/0379-6787(91)90076-2
9. M. de la L. Olivera, A. Maldonado, R. Asomoza, O. Solorza, D.R. Acosta, Thin Solid Films **394**, 242 (2001)
10. M. de la L. Olivera, A. Maldonado, R. Asomoza, Solar Energy Mat. Solar Cell **73**, 425 (2002). DOI 10.1016/S0927-0248(02)00211-8
11. T. Miyata, S. Ida, T. Minami, J. Vac. Sci. Technol. A **21**(4), 1404 (2003). DOI 10.1116/1.1580492
12. T. Minami, S. Ida, T. Miyata, Y. Minamoto, Thin Solid Films **445**, 268 (2003). DOI 10.1016/S0040-6090(03)01159-3
13. H.Y. Xu, Y.C. Liu, R. Mu, C.L. Shao, Y.M. Lu, D.Z. Shen, X.W. Fan, Appl. Phys. Lett. **86**, 123107–1 (2005). DOI 10.1063/1.1884256
14. R.G. Gordon, MRS Bull. **25**(8), 52 (2000)
15. R.C. Weast, M.J. Astle, *Handbook of Chemistry and Physics*, 61th edn. (CRC, Boca Raton, 1980–1981), pp. B-164
16. Y. Shigesato, N. Shin, M. Kamei, P.K. Song, I. Yasui, Jpn. J. Appl. Phys. **29**, 6422 (2000). DOI 10.1143/JJAP.39.6422
17. K.S. Lee, T.S. Lee, I.H. Kim, B. Cheong, W.M. Kim, Integr Ferroelectr **69**, 295 (2005). DOI 10.1080/10584580590899045
18. B. Stjerna, E. Olsson, C.G. Granqvist, J. Appl. Phys. **76**, 3797 (1994). DOI 10.1063/1.357383
19. R. Cebulla, W. Wendt, K. Ellmer, J. Appl. Phys. **83**, 1087 (1998). DOI 10.1063/1.366798
20. A. Sanchez-Juareza, A. Tiburcio-Silverb, A. Ortizc, E.P. Zironid, J. Rickards, Thin Solid Films **333**, 196 (1998). DOI 10.1016/S0040-6090(98)00851-7
21. A.F. Kohan, G. Ceder, D. Morgan, C.G. Van de Walle, Phys. Rev. B **61**, 15019 (2000). DOI 10.1103/PhysRevB.61.15019
22. K. Ellmer, J. Phys. D: Appl. Phys. **33**, R17 (2000). DOI 10.1088/0022-3727/33/4/201
23. L.E. Brus, J. Chem. Phys. **80**, 4403 (1984). DOI 10.1063/1.447218
24. T. Senda, Y.-J. Cho, T. Hirakawa, H. Okamoto, H. Takakura, Y. Hamakawa, Jpn. J. Appl. Phys. **39**, 4716 (2000). DOI 10.1143/JJAP.39.4716
25. S.A. Knickerbocker, A.K. Kulkarni, J. Vac. Sci. Technol. A, **13**, 1048 (1995). DOI 10.1116/1.579583